Documentation for AECL Lidar data release for the ESCAPE flight campaign 2022

1 July 2023

Prepared by: Dr. Keyvan Ranjbar, Mr. Kenny Bala

Reviewed by: Dr. Mengistu Wolde

Ver. 1.0

NRC Convair AECL 355 lidar system

Airborne Elastic Cloud Lidar (AECL) built by Alpenglow, Inc. is a compact single wavelength airborne elastic lidar operating at 355nm and used for the retrieval of vertical profiles of atmospheric properties, such as scattering and extinction properties of clouds and aerosols. In 2014 the NRC purchased Zenith AECL system for the installation on the Convair-580 airborne platform. The approximate locations of the lidar is shown in Figure 1.

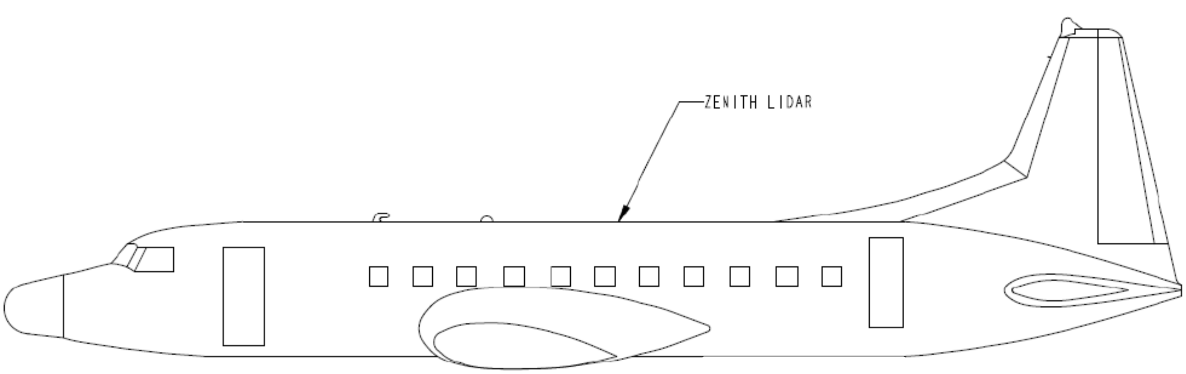

Figure 1: Approximate locations of the AECL zenith system on board the Convair-580 aircraft.

The AECL lidar design is shown in Figure 2 while its main technical specifications are listed in Table 1. Additional details regarding AECL technical specifications can be found in Baibakov et. al. (2016, 2018).

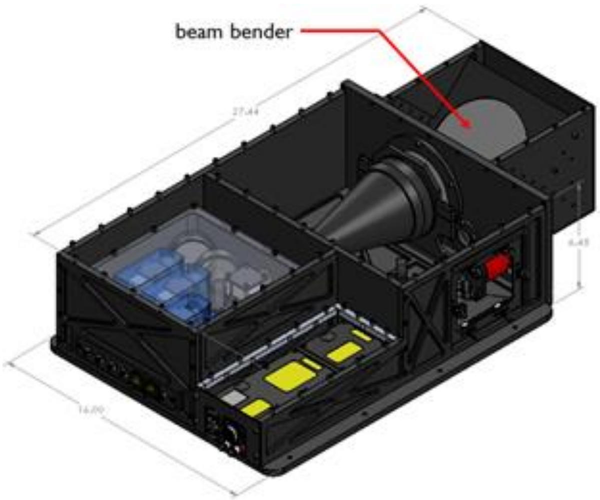

Figure 2: Left: AECL CAD model with dimensions specified in inches. Right: AECL when installed in zenith configuration on board the Convair-580 aircraft.

Table 1. Technical specifications of the AECL transmitter, receiver and data acquisition system

Transmitter	
Laser Wavelength	355nm YAG
Pulse Repetition Frequency	20 Hz
Pulse Width	≈8 ns
Pulse Energy	12mJ
Beam Divergence	0.4×10^{-3} radians
Receiver	
Diameter	≈100 mm
Field of View	≈1000 µrad
Data System	
Number of Channels	Four: Low and high gain parallel and perpendicular signals
Detector	PMT
Range Resolution	1.5m, 3.0m, 6.0m, 12m (programmable)

AECL data acquisition statistics during the ESCAPE

Table 2 shows AECL data acquisition statistics during the ESCAPE.

Table 2. AECL data acquisition during ESCAPE

Flight	***Date***	***Start***	***End***	***Duration***	***Coverage***
C-RF01	31 May, 2022	14:09	18:36	4h27	
C-RF02	02 June, 2022	15:05	19:22	4h17	
C-RF03	02 June, 2022	21:15	01:18	4h03	
C-RF04	04 June, 2022	18:55	23:00	4h05	
C-RF05	08 June, 2022	14:55	19:05	4h10	
C-RF06	09 June, 2022	19:55	00:08	4h13	
C-RF07	10 June, 2022	20:12	00:50	4h38	
C-RF08	11 June, 2022	19:40	00:22	4h44	
C-RF09	12 June, 2022	17:10	21:46	4h36	
C-RF10	14 June, 2022	17:10	21:38	4h28	
C-RF11	16 June, 2022	15:03	19:19	4h16	
C-RF12	16 June, 2022	20:43	01:08	4h25	
C-RF13	17 June, 2022	15:00	19:38	4h38	

75 - 100%	50 -74%	20 - 50%	< 20%

This percentages only refers to data coverage, not data quality

AECL data processing

The detailed description of AECL data processing can be found in Baibakov et al, 2019. In short, there are several levels of processing. Low level processing consists of a background subtraction and a range correction. The former ensures that the signal is zero when no laser return is being registered while the latter corrects for the signal drop off as the laser pulse propagates away from the emitter.

Once the low-level processing is completed, the lidar return is corrected for altitude. The altitude correction is needed to transform the relative height above/below aircraft to absolute altitudes above mean sea level which is done using the data from aircraft sensors.

Depolarization

AECL can estimate a degree of particle-induced depolarization of the emitted laser pulse by separately measuring parallel and perpendicular polarization components of the return signal, $P_{\parallel}$ and $P_{\perp}$. The ratio of the measured cross-polarized power ($P_{\perp}$) to the co-polarized power, ($P_{\parallel}$) is defined as the linear depolarization ratio, LDR :

$$LDR = \frac{P_{\perp}}{P_{\parallel}}$$

LDR can often provide an insight into the types of particles encountered by the laser beam, with lower LDR values often associated with spherical particles, most often liquid drops.

Since this Lidar is a cloud lidar and the power is low, usually it is not very sensitive to aerosol but in the ESCAPE 2022 campaign during flight C-RF09 and C-RF10, dust activities in the AECL Lidar backscatter and depolarization profiles had been observed. (Ranjbar et. al., 2023)

Example of lidar measurements during the ESCAPE

Figure 3 shows an example of AECL measurements made between 18:45 and 19:00 during flight C-RF11 on Jun. 16, 2022. The top and bottom panes show vertical profiles of uncalibrated lidar (co-polarized) return and linear depolarization ratio respectively.

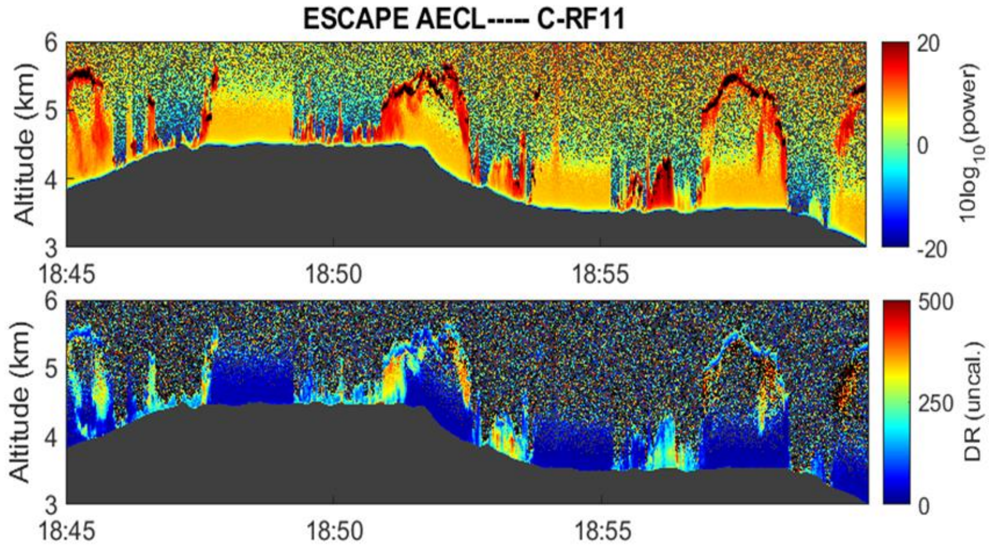

Figure 3: AECL uncalibrated return (top) and depolarization ratio (bottom) during flight C-RF11 on Jun. 16, 2022.

Dataset structure

Here we describe the variables of the AECL lidar datasets.

Variables:

time

Dimensions: time

Datatype: double

Attributes:

long_name = **'time of measurement'**

units = 'seconds since 1970-01-01T00:00:00 +0000'

range

Dimensions: range

Datatype: double

Attributes:

Long name = **'Range bins above the aircraft'**

Unit = 'km'

lat

Dimensions: time

Datatype: double

Attributes:

long_name = **'Aircraft latitude from KVH1750 IMU, in units of degrees North'**

units = 'deg'

comments = 'Data produced by combining GPS and IMU observations via a Kalman Filter in real time'

lon

Dimensions: time

Datatype: double

Attributes:

long_name = **'Aircraft longitude from KVH1750 IMU, in units of degrees East'**

units = 'deg'

comments = 'Data produced by combining GPS and IMU observations via a Kalman Filter in real time'

alt

Dimensions: time

Datatype: double

Attributes:

long_name = **'Aircraft altitude from KVH1750 IMU, in units of metres'**

units = 'm'

comments = 'Data produced by combining GPS and IMU observations via a Kalman Filter in real time'

CoPolHi

Dimensions: time,range

Datatype: double

Attributes:

Long name = **'Co-Polarized High Gain'**

Unit = 'Uncalibrated power'

CrossPolHi

Dimensions: time,range

Datatype: double

Attributes:

Long name = **'Cross-Polarized High Gain'**

Unit = 'Uncalibrated power'

DRHi

Dimensions: time,range

Datatype: double

Attributes

Long name = **'Depolarization ratio CoPol/CrossPol (uncalibrated)'**

Unit = 'Unitless'

References

- Baibakov, K., Wolde, M., Nguyen, C. and Korolev, A., (2019), Airborne elastic cloud lidar for ice-water content retrievals during the HAIC-HIWC 2015 campaign, NRC technical report, 58 p., doi: 10.5281/zenodo.3585578.
- Baibakov, K., Wolde, M., Nguyen, C., Korolev, A., Wang, Z., and Wechsler, P., (2016), Performance of a compact elastic 355 nm airborne lidar in tropical and mid-latitude clouds, Proc. SPIE 10006, Lidar Technologies, Techniques, and Measurements for Atmospheric Remote Sensing XII, 100060C; https://doi.org/10.1117/12.2242112

- Baibakov, K., Wolde, M., Nguyen, C., Korolev, A., Heckman, I., (2018), Retrievals of ice-water content from an airborne elastic lidar in tropical convective clouds, EPJ Web Conf. 176 0505; https://doi.org/10.1051/epjconf/201817605051
- Ranjbar, K., Nichman, L., McFarquhar, G., Wolde, M., Kollias, P. and Bala, K., (2023), Assessing optical measurements of Saharan dust in the ESCAPE 2022 campaign. IUGG general assembly